JOURNAL OF CATALYSIS **165,** 241–248 (1997)
ARTICLE NO. CA971473

Isomerization and Hydrocracking of Heptane over Bimetallic Bifunctional PtPd/H-Beta and PtPd/USY Zeolite Catalysts

E. Blomsma, J. A. Martens,[1] and P. A. Jacobs

Centrum voor Oppervlaktechemie en Katalyse, Katholieke Universiteit Leuven, Kardinaal Mercierlaan 92, B-3001 Leuven (Heverlee), Belgium

Received June 18, 1996; revised September 19, 1996; accepted September 30, 1996

Bifunctional catalysts are prepared by loading NH_4-Beta zeolites with platinum, palladium, and platinum–palladium metal combinations via cation exchange and incipient wetness impregnation with $Pt(NH_3)_4Cl_2$ and $Pd(NH_3)_4Cl_2$ complexes, followed by calcination and reduction. In comparison to the Pt and Pd loaded acid zeolites, the bimetallic Pd–Pt zeolites are found to be more active and selective in the isomerization of heptane. The noble metal phases are characterized with temperature programmed reduction and hydrogen chemisorption. The dispersion of platinum is significantly improved in presence of as little as 20 mole% of palladium. The improved Pt dispersion leads to a better intimacy and balance of the acid and hydrogenation–dehydrogenation functions in these bifunctional catalysts and suppression of undesirable hydrogenolysis and dimerization-cracking activity. On Pt/USY zeolite, the addition of palladium has similar beneficial effects on the catalytic performances.

INTRODUCTION

Bifunctional catalysis refers to the operation of catalysts comprising a combination of acid and hydrogenation-dehydrogenation functions (1–4). The acidity is typically provided by a zeolite, while the hydrogenation–dehydrogenation activity is exerted by finely dispersed platinum or palladium metal. Bifunctional catalysis with zeolites plays an important role in petroleum refining and is applied in processes such as hydrocracking, isomerization, and catalytic dewaxing (5).

The conventional reaction mechanism for the conversion of an alkane on a bifunctional catalyst has been described originally by Coonradt and Garwood (1) and Weisz (2). The metal phase dehydrogenates the alkanes into alkenes which are protonated at the Brønsted acid sites yielding alkylcarbenium ions. After rearrangements and/or scissions, these alkylcarbenium ions desorb from the acid sites as alkenes and are hydrogenated at the metal phase to yield saturated reaction products (1, 2). The synergism between the two catalytic functions has been demonstrated with physical mixtures of monofunctional catalyst pellets containing the acid and noble metal, respectively (2). In order to avoid that the reaction rate is limited by alkene transport, the catalytic functions need to be at short mutual distances. An *intimacy criterion* (2) can be handled to verify whether the condition of intimacy between the two types of catalytic sites is fulfilled:

$$R_c^2 < 1.2 \times 10^5 \frac{P_0 \cdot D_0}{T \cdot dN/dt}. \quad [1]$$

In this expression, P_0 (MPa) is the partial pressure of the alkene intermediate, T (K) the temperature, R_c (m) the radius of the catalyst particles (which is a measure for the spacial separation of the functions), D_0 ($m^2 \cdot s^{-1}$) the diffusivity of the alkenes in the catalyst pores and dN/dt ($mol \cdot s^{-1} \cdot m^{-3}$) the intrinsic reaction rate of acid catalyzed alkene conversion. This *intimacy criterion* is rather insensitive to particle shape and exact kinetics (2). The realization of sufficient intimacy in zeolites is critical due to the slow micropore diffusion of the hydrocarbons in the zeolite micropores and the high catalytic turnover numbers of the acid sites (6).

The conventional bifunctional reaction mechanism is operative, provided the condition of intimacy is met and the hydrogenation–dehydrogenation activity of the catalyst is sufficient to balance the acidity (3). Under such conditions, the rearrangements of the alkylcarbenium ions are the rate limiting steps of the reaction scheme. Depending on the zeolite type, these rearrangements may be subjected to molecular shape selective effects in the micropores (7).

Quantification of the condition of balance between acid and metal functions is not straightforward. Guisnet *et al.* (8, 9) studied the conversion of heptane on Pt/H-Y zeolite catalysts and attempted to quantify the balance of the functions in terms of numbers of strong acid sites of which the adsorption enthalpy for ammonia exceeds 100 kJ/mol and numbers of accessible noble metal atoms as counted by hydrogen chemisorption. At high metal content (more

[1] Correspondence and reprint requests should be addressed to Dr. J. A. Martens, Centrum voor Oppervlaktechemie en Katalyse, Kardinaal Mercierlaan 92, B-3001 Heverlee, Belgium. Tel: (32)16-321637; FAX: (32)16-321998; E-mail: johan.martens@agr.kuleuven.ac.be.

0021-9517/97 $25.00

than one Pt atom per six strong acid sites), the catalyst is capable of isomerizing heptane in the absence of cracking. The following sequence of reaction products is observed at increasing reaction severity: heptane ⇒ methylhexanes ⇒ dimethylpentanes ⇒ cracked products (8). A catalyst exhibiting this reaction sequence is considered to be in balance, as the product distributions reflect consecutive transformations of alkylcarbenium ion intermediates (10). With well-balanced catalysts only, heptane can be selectively isomerized into its monobranched skeletal isomers. The selectivity of heptane for dibranching is likewise dependent on the balance of the catalytic functions but is much lower than for monobranching because of the fast cracking of these specific isomers.

In previous work, we studied the isomerization and hydrocracking of heptane on Pt/H-Beta and Pd/H-Beta zeolites loaded with different amounts of Pd or Pt metal (0.05 to 1.5 wt%) and with different metal dispersions obtained by altering the metal loading technique (impregnation, cation exchange, competitive cation exchange) (11–13). On these catalysts, heptane is converted mainly according to the conventional bifunctional mechanism, but bimolecular mechanisms and, with Pt/H-Beta, metal catalyzed cracking (hydrogenolysis) were superimposed. The bimolecular mechanism leads to isoheptanes as well as cracked products via dimerization of the alkene intermediates on the acid sites and recracking (11). Among the isoheptanes, the bimolecular mechanism selectively produces 2-methylhexane, 3-methylhexane, 2,3-dimethylpentane, and 2,4-dimethylpentane (12), while the conventional mechanism can produce all individual heptane isomers, including *gem*-dimethylbranched and ethylbranched isomers (14). Any C_3^+ cracked product including compounds with five and six carbon atoms can be produced via the bimolecular mechanism (8, 11, 15, 16).

In Pd/H-Beta catalysts, the bimolecular mechanism can only be suppressed by increasing the Pd content of the catalyst (11, 12). With Pt/H-Beta catalysts, the bimolecular mechanism is less important, but the catalyst promotes hydrogenolysis as platinum is a more active hydrogenation–dehydrogenation catalyst compared to palladium (13). Even at a Pt loading of 1.5 wt% and 80% Pt dispersion, hydrogenolysis and bimolecular reactions are still superimposed on the conventional mechanism (13). This behavior of zeolite Beta was ascribed to its strong acidity, which is intermediate between that of Y-type zeolites and sulfated zirconia (12).

Virtually any property of a dispersed metal catalyst may be influenced by the addition of a second metal to form bimetallic clusters (17). In a variety of reactions, alloying of platinum with other metals results in a beneficial effect on catalytic performance (18). Alloying of the platinum surface generates very small ensembles of surface platinum atoms, in the same way as reduction of the metal particle size does (19–21). For example, a bimetallic platinum–rhenium on chlorinated alumina catalyst in naphta reforming enables the operation at lower pressures, is more stable, and yields a better product quality, compared to a platinum catalyst (18, 22).

In this work, we investigated the isomerization and hydrocracking of heptane on H-Beta and USY zeolite catalysts, containing both platinum and palladium metal. It was found that the combination of the two metals in a bifunctional zeolite leads to superior catalytic performances with respect to isomerization yield. With the Pd–Pt metal combination, bimolecular reactions are suppressed and the hydrogenolysis activity eliminated. Temperature programmed reduction and chemisorption are used to characterize these bimetallic catalysts and to explain their catalytic behavior.

EXPERIMENTAL

Catalyst preparation. H-Beta zeolite (PQ Corporation, sample PQ304 type CBV811) was characterized by a Si/Al ratio of 12.5, a B.E.T. surface area of 750 m^2/g, and crystal size between 0.1 and 0.7 μm. The ultrastable Y zeolite (PQ Corporation, sample PQ300 type CBV712) had a Si/Al ratio of 5.45, a surface area of 730 m^2/g, and crystal size between 0.2 and 0.5 μm. The H-Beta and USY zeolites were converted into their ammonium form by contacting the powders with aqueous ammonia solutions at pH 9. The noble metals were introduced using incipient wetness impregnation *[IM]* or cation exchange *[EX]* with aqueous solutions of $Pt(NH_3)_4Cl_2$ and/or $Pd(NH_3)_4Cl_2$ (Johnson Matthey). In the cation exchange operations, the liquid/solid ratio in the slurries was 200 ml per gram of zeolite. After ion exchange, the zeolite crystals were recovered by filtration. Quantitative uptake of the metals occurred in all instances, as verified with atomic absorption spectroscopy on the filtrates. Noble metal loadings are expressed in weight percent (wt%) on a dry zeolite weight basis.

Catalytic testing. Catalyst pellets with diameters from 0.3 to 0.8 mm were prepared by compressing the zeolite powders into flakes, followed by crushing and sieving. Typically 500 mg of catalyst pellets was loaded into the reactor tube (internal diameter of 1 cm), activated in flowing oxygen at a space time W/F_0 (W = catalyst weight, F_0 = molar flow at reactor inlet) of $8 \cdot 10^{-3}$ h · kg · mol^{-1}, using a temperature increase of 10°C per minute to 400°C. After 1 h at 400°C, the catalyst bed is flushed with nitrogen and contacted with flowing hydrogen at the same space time for another hour. The catalyst was cooled under hydrogen to the reaction temperature. In the catalytic experiments, the total pressure in the reactor was 0.3 MPa and the molar hydrogen/heptane ratio in the feed was 60. The space time was adjusted to reach a heptane conversion of 82.5%. The reaction products were analyzed on-line with a HP5890II

gaschromatograph, equipped with a 50m CPSil5 column (Chrompack) and an FID detector.

The yield of a cracked product fraction with carbon number i, Y^*_{Ci}, is calculated on a mol/100 mol of cracked heptane basis from the following equation (8):

$$Y^*_{Ci} = \left(\frac{1}{i} \sum_{j=1}^{n_j} A_{i,j} \Big/ \frac{1}{7} \sum_{i=1}^{6} \sum_{j=1}^{n_j} A_{i,j} \right) \times 100 \quad (\text{mol}/100\,\text{mol}) \qquad [2]$$

in which $A_{i,j}$ represents the peak area in the chromatogram of reaction product j with carbon number i and n_i the number of reaction products with carbon number i.

The following equations have been used to estimate the contribution of hydrogenolysis (Hy), monomolecular (HC) and bimolecular (DC) hydrocracking (8, 11):

$$HC = 100\,(2Y^*_{C3}) \Big/ \sum_{i=1}^{6} Y^*_{Ci} \quad (\%\ \text{of total}\ C_7\ \text{cracking}) \qquad [3]$$

$$Hy = 100\,(2 \cdot Y^*_{C1} + 2 \cdot Y^*_{C2}) \Big/ \sum_{i=1}^{6} Y^*_{Ci} \quad (\%\ \text{of total}\ C_7\ \text{cracking}) \qquad [4]$$

$$DC = 100\,(Y^*_{(C4+C5+C6)} - Y^*_{C1} - Y^*_{C2} - Y^*_{C3}) \Big/ \sum_{i=1}^{6} Y^*_{Ci} \quad (\%\ \text{of total}\ C_7\ \text{cracking}). \qquad [5]$$

In Eq. [3] the contribution of monomolecular hydrocracking (HC) is estimated as the molar yield of C_3 and an equimolar yield of C_4. Scissions into fragments with other carbon numbers are unlikely according to alkylcarbenium ion chemistry (6). Methane and ethane are typical hydrogenolysis products. The contribution of hydrogenolysis is estimated based on the yields of methane, ethane, and equimolar amounts of C6 and C5 products, respectively (Eq. [4]). The contribution of dimerisation-cracking (bimolecular hydrocracking) is estimated as the excess molar yield of C4, C5, and C6 with respect to C1, C2, and C3 products (Eq. [5]). These HC, Hy, and DC values represent an estimation of the contribution of these cracking mechanisms, useful in a discussion of the impact of catalyst modification (8, 11).

The catalytic activity (A) has been calculated as a space-time-product-yield:

$$A = 0.10 \times \frac{X_{feed}}{W/F_0} \quad (\text{mol} \cdot \text{h}^{-1} \cdot \text{kg}^{-1}). \qquad [6]$$

Temperature programmed reduction and metal dispersion measurements. The outlet of a small fixed bed reactor was coupled with an SX200 quadrupole mass spectrometer from VG instruments. A secondary electron multiplier was used to enhance the sensitivity.

Metal dispersions were measured using hydrogen chemisorption. The catalyst was pretreated as for the catalytic experiments. Prior to the chemisorption experiments, hydrogen was desorbed at 400°C under flowing helium. Chemisorptions were carried out at room temperature. Pulses (20 μl) of an equimolar mixture of hydrogen and argon were injected into a stream of helium carrier gas flow ($W/F_0 = 0.01\ \text{h} \cdot \text{kg} \cdot \text{mol}^{-1}$) and contacted with the catalyst. Argon was used as a tracer to enable the counting of the adsorbed hydrogen pulses. In the calculation of the dispersion, it was assumed that every surface atom of platinum chemisorbs one hydrogen atom. The dispersions, d (%) were calculated as the number of platinum atoms at the surface divided by the total number of platinum atoms in the sample.

For the calculation of the average metal particle diameter, a spherical particle shape was adopted. The average diameter of platinum spheres, D (nm), was calculated from the equation (13)

$$D = 5.21 \times 10^3\ MG^{-1} \quad (\text{nm}) \qquad [7]$$

in which M (g) represents the weight of platinum in the sample and G (μmol), the number of hydrogen atoms adsorbed.

In the bimetallic catalysts, palladium was assumed to behave like platinum and Eq. [7] was adapted accordingly.

In the TPR experiments, calcined zeolites were contacted with a 5% of hydrogen in nitrogen mixture ($W/F_0 = 0.01\ \text{h} \cdot \text{kg} \cdot \text{mol}^{-1}$) at a heating rate of 10°C per minute.

RESULTS AND DISCUSSION

Heptane Conversion on PtPd/H-Beta and PtPd/H-USY Catalysts

A first series of catalysts contained 0.5 or 1.0 wt% of platinum and different amounts of palladium. On the Beta zeolites, the metals were introduced by cation exchange. The USY zeolites were loaded with noble metals using co-impregnation. Heptane was converted at a reaction temperature of 232°C, and the contact time adjusted to reach 82.5% of heptane conversion. The behavior of these catalysts in heptane conversion is reported in Fig. 1 and Table 1. On *0.50 $Pt^{(EX)}$H-Beta* and *1.00 $Pt^{(EX)}$H-Beta*, the isomerization yield increases with the Pd content of the catalyst varying 0 to 0.50 wt% (Fig. 1a). The hydrogenolysis activity decreases with increasing Pd content and has vanished in the catalysts containing 0.50 wt% Pd (Fig. 1c). On H-Beta containing 0.50 wt% of Pd and 0.50 or 1.0 wt% of Pt, the heptane isomerization yield reaches the highest values obtained (ca. 75%). With increasing Pd addition, the yield of multibranched isoheptanes tends to increase (Fig. 1b) and the contribution of dimerization-cracking mechanisms

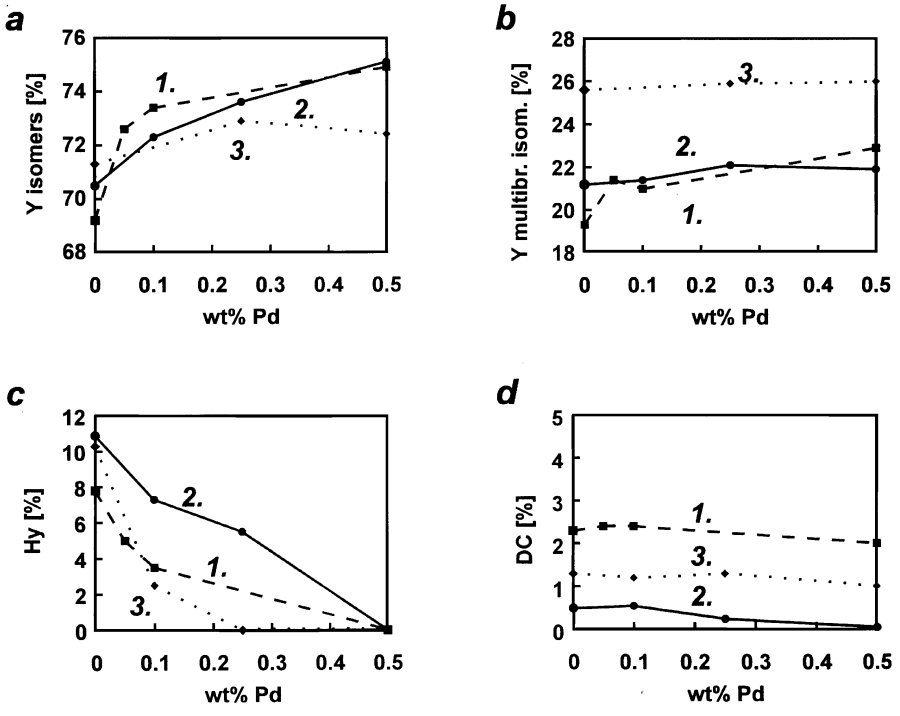

FIG. 1. Yield of C_7 isomers ***(a)***, multibranched C_7 isomers ***(b)***, hydrogenolysis ***(c)***, and dimerization-cracking ***(d)*** in heptane conversion on *0.50 $Pt^{[EX]}$H-Beta* ***(1)***, *1.00 $Pt^{[EX]}$H-Beta* ***(2)***, and *1.00 $Pt^{[IM]}$USY* ***(3)*** containing various amounts of Pd (T = 232°C; P = 0.3 MPa; $H_2/C_7 = 60$; $X_{C7} = 82.5\%$).

to decrease (Fig. 1d). The dimerization-cracking activity of H-Beta zeolites containing 1.0 wt% of Pt is systematically lower than at 0.5 wt% Pt loading (Fig. 1d), as expected for a better acid/metal balance. Pd addition does not eliminate this difference. On the *1.0 Pt 0.5 $Pd^{[EX]}$H-Beta* catalyst, heptane can be converted in absence of hydrogenolysis and dimerization-cracking (Figs. 1c and 1d).

The influence of the reaction temperature on the isomerization and hydrogenolysis of heptane on bimetallic H-Beta zeolites is illustrated in Fig. 2. The changes in catalytic behavior upon Pd addition to Pt/H-Beta, observed at 232°C (Fig. 1), are also observed in a broader temperature window from 207 to 237°C (Fig. 2). The reduction of the hydrogenolysis activity upon Pd addition is most pronounced at low reaction temperatures (Fig. 2).

The C_7 isomer distributions obtained on Pt/H-Beta and PtPd/H-Beta catalysts at 232°C are detailed in Table 1. The distribution of monobranched isomers obtained on the different catalysts is very similar and reflects the thermodynamic equilibrium among these isomers (14).

TABLE 1

Distribution (mol%) of Mono- and Multibranched Isomers Obtained from Heptane Conversion on *0.50 $Pt^{[EX]}$H-Beta*, *1.00 $Pt^{[EX]}$H-Beta* and *1.00 $Pt^{[IM]}$H-USY* with and without Addition of Pd (Reaction Conditions of Fig. 1)

		Monobranched isomers (%)			Multibranched isomers (%)		
Metal loading	Zeolite	$2MeC_6$	$3MeC_6$	$3EtC_5$	2,2 + 3,3 $diMeC_5$	2,3 + 2,4 $diMeC_5$	2,2,3 $tri\text{-}MeC_5$
0.5 Pt	H-Beta	48.3	48.2	3.5	33.8	64.4	1.8
0.5 Pt 0.1 Pd	„	48.4	48.0	3.6	38.9	59.5	1.4
0.5 Pt 0.5 Pd	„	48.4	48.2	3.4	40.6	57.8	1.6
1.0 Pt	H-Beta	48.3	48.3	3.4	40.4	57.9	1.6
1.0 Pt 0.25 Pd	„	48.3	48.4	3.3	40.6	57.8	1.6
1.0 Pt 0.5 Pd	„	48.1	48.3	3.6	40.9	57.7	1.4
1.0 Pt	H-USY	47.8	48.9	3.4	44.2	52.5	3.3
1.0 Pt 0.25 Pd	„	47.6	49.0	3.4	43.6	53.0	3.4
1.0 Pt 0.5 Pd	„	47.6	49.1	3.3	42.3	54.5	3.3

Note. T = 232°C; P = 0.3 Mpa; $X_{C7} = 82.5\%$; $H_2/C_7 = 60$.

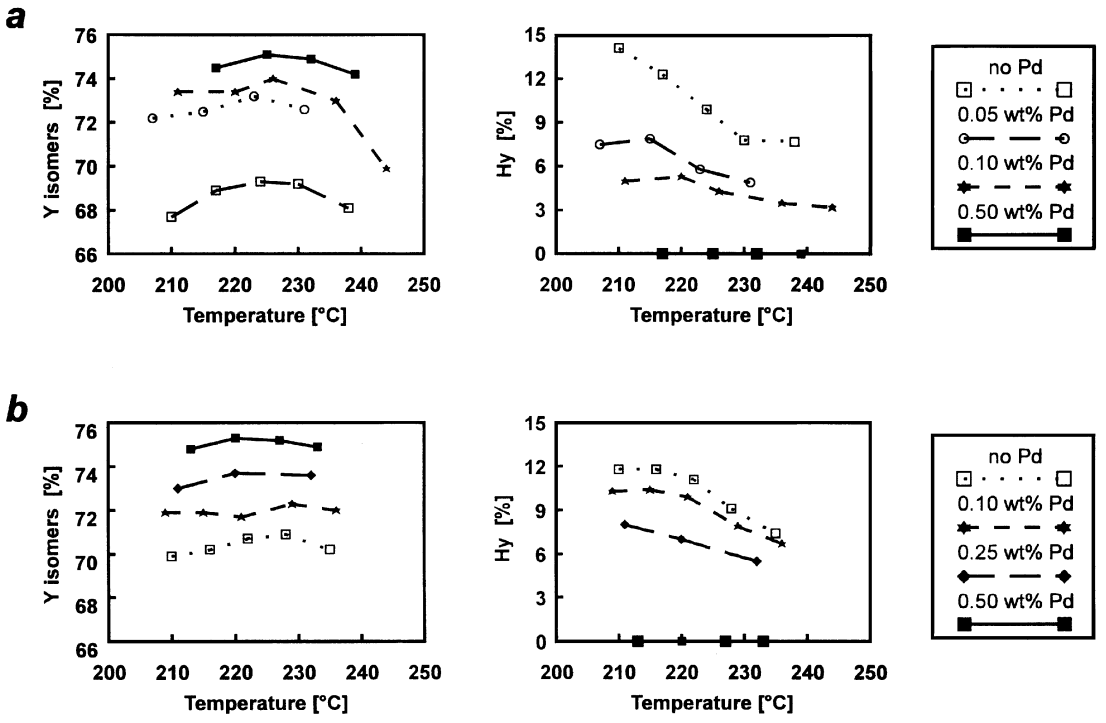

FIG. 2. Yield of C_7 isomers and contribution of hydrogenolysis in heptane conversion at different reaction temperatures on *0.50 $Pt^{[EX]}$H-Beta* ***(a)*** and *1.00 $Pt^{[EX]}$H-Beta* ***(b)*** containing various amounts of Pd ($P = 0.3$ MPa; $H_2/C_7 = 60$; $X_{C7} = 82.5\%$).

Addition of 0.1 wt% of Pd to *0.50 $Pt^{[EX]}$H-Beta* results in an enhanced formation of *gem*-dimethylbranched isoheptanes (2,2- and 3,3-dimethylpentane) among the multibranched isoheptanes, indicating that the contribution of the bimolecular isomerization mechanism has become less important. Addition of more Pd to *0.50 $Pt^{[EX]}$H-Beta* or Pd addition to *1.0 $Pt^{[EX]}$H-Beta* does not significantly alter the distribution of multibranched isomers.

The behavior of the USY zeolite is quite similar to H-Beta, but less Pd seems to be necessary to reach the optimum catalytic performance. Addition of 0.25 wt% Pd to the *1.00 $Pt^{[IM]}USY$* formulation eliminates the hydrogenolysis activity (Fig. 1c) and results in an improved isomerization yield (Fig. 1a). Addition of more Pd does not further improve the isomerization yield (Fig. 1a). It has a small beneficial effect on the yield of multibranched isomers (Fig. 1b), and it slightly decreases the dimerization-cracking contribution (Fig. 1d).

The systematically lower amount of 2,2,3-trimethylbutane in the multibranched isomers obtained on Beta zeolites compared to USY (Table 1) is ascribed to a molecular shape selective effect (12).

A second series of H-Beta and USY catalysts has been prepared using the ion exchange technique aiming at a constant total weight loading of 0.50 wt% noble metals and varying the Pt/Pd proportions. The atomic Pd/(Pt + Pd) ratio was varied between 0 and 1.

The total C_7 isomer yield, the yield of multibranched C_7 isomers, and the contributions of hydrogenolysis and dimerization-cracking at 82.5% heptane conversion on 0.50 wt% PtPd/H-Beta and USY catalysts with different Pt–Pd compositions is reported in Fig. 3. On both types of zeolites, an optimum atomic Pd/(Pt + Pd) ratio around 0.3–0.4 exists

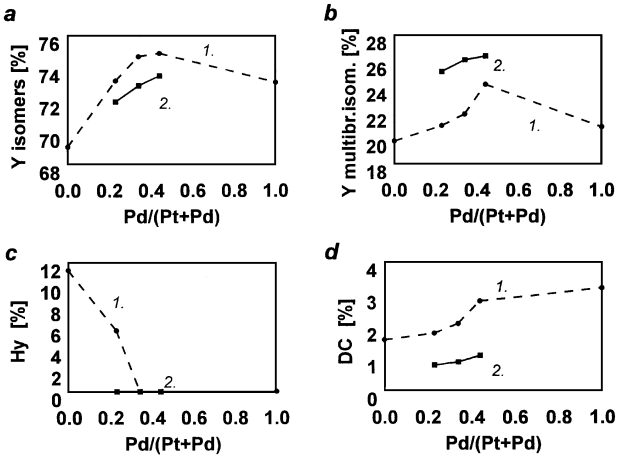

FIG. 3. Total C_7 isomer yield ***(a)***, yield of multibranched C_7 isomers ***(b)***, and contribution of hydrogenolysis ***(c)*** and dimerization-cracking ***(d)*** on *H-Beta$^{[EX]}$* ***(1)*** and *USY$^{[IM]}$* ***(2)*** zeolites loaded with 0.5 wt% of noble metal and a variable Pd fraction ($T = 220$°C (H-Beta) or 232°C (USY); $X_{C7} = 82.5\%$).

TABLE 2

Catalytic Activity (A) and Yield of Isomerization (Yiso) with Monometallic Pt and Bimetallic Pt–Pd/H-Beta and USY Catalysts in Heptane Conversion

Catalyst	T [°C]	A [mol · h^{-1} · kg^{-1}]	Yiso [%]
0.50 $Pt^{(EX)}$H-Beta	225	9.5	69.3
0.50 Pt 0.10 $Pd^{(EX)}$H-Beta	225	13.1	74.0
0.43 Pt 0.07 $Pd^{(EX)}$H-Beta	225	13.6	74.8
0.50 $Pd^{(IM)}$H-Beta	225	9.8	73.1
1.00 $Pt^{(EX)}$H-Beta	218	7.0	70.5
1.00 Pt 0.10 $Pd^{(EX)}$H-Beta	218	12.1	72.3
1.00 $Pt^{(EX)}$USY	235	2.1	71.3
1.00 Pt 0.10 $Pd^{(EX)}$USY	235	2.5	73.2

Note. P = 0.3 MPa; $X_{C7} = 82.5\%$; $H_2/C_7 = 60$.

at which the highest yield of total C_7 isomers and multibranched C_7 isomers is reached (Figs. 3a and b). Bimetallic 0.50 wt% PtPd/H-Beta and USY catalysts do not exhibit hydrogenolysis (Fig. 3c). Their dimerization-cracking activity increases slightly with increasing Pd fraction (Fig. 3d).

The catalytic activity of the bimetallic catalysts is higher than that of the monometallic Pt and Pd catalysts (Table 2).

Redox Chemistry of Bimetallic Bifunctional Zeolites

From literature it is known that the activation procedure of zeolites exchanged with platinum tetrammine complex is quite critical. The typical procedure for obtaining a dispersed Pt metal phase comprises calcination in air or oxygen followed by a reduction in hydrogen. At low calcination temperatures or at low oxygen partial pressures during calcination, autoreduction of the metal by its ammonia ligands may occur. In the subsequent reduction step in hydrogen, a neutral volatile species with chemical composition $Pt(NH_3)_4H_2$ is formed which tends to agglomerate and finally gives rise to the formation of very large platinum metal particles outside the zeolite crystals (23, 24).

After oxidative treatment of the catalyst precursor, platinum may occur as Pt^{2+} or Pt^{4+} cations balancing zeolite lattice charges, or else as PtO or PtO_2 oxides, depending on the zeolite type and oxidation conditions (23, 25–27). Chmelka *et al.* provided experimental evidence (using Raman spectroscopy and ^{129}Xe-NMR) that during calcination of Pt/Na,H-Y at 400°C, PtO is formed (28, 29). Calcination temperatures above 500°C lead to decomposition of the PtO phase, producing Pt^{2+} cations, while calcination at temperatures below 400°C leads to incomplete removal of the ammonia ligands with detrimental consequences for the metal dispersion (28, 29). Ostgard *et al.* found that Pt/K-L zeolite catalysts, on which platinum was introduced via cation exchange, contain PtO particles after calcination at 400°C (30). However, if incipient wetness impregnation is used to deposit Pt on the K-L zeolite, predominantly Pt^{4+} cations with a minority of Pt^{2+} cations are obtained after calcination at 400°C. After reduction, the Pt particles of the $Pt^{[IM]}K$-*L* catalyst are located inside the channels, while in the $Pt^{[EX]}K$-*L* sample, part of the Pt metal is located on the external surface of the zeolite crystals (30).

Ammonium-exchange of the zeolite and deammoniation at elevated temperature is a current technique to generate Brønsted acidity. Upon calcination of zeolites exchanged with ammonium and platinum cations such as Pt/NH_4-L (30) and Pt/NH_4-Beta (31), reduction of the platinum by the ammonia can occur and can give rise to very low platinum dispersions (32). Calcination in pure oxygen using short space time and small heating rates was found to be an effective method to avoid this reduction (31).

The reduction with hydrogen of calcined 0.50 $Pt^{[EX]}$H-Beta and 0.50 $Pt^{[EX]}$USY zeolites and Pd containing versions was studied with TPR experiments in which the hydrogen consumption and the formation of water was monitored (Fig. 4). All samples produced water upon reduction, indicating that after calcination, metal oxides were present. On Pt/H-Beta and Pt/USY zeolites, the consumption of hydrogen and the formation of water start at a temperature at ca. 300°C (Fig. 4). On the palladium containing Beta sample, the reduction starts at a lower temperature of ca. 200°C. With Pd–Pt combinations, a reduction step starting at ca. 250°C is observed, the low temperature reduction

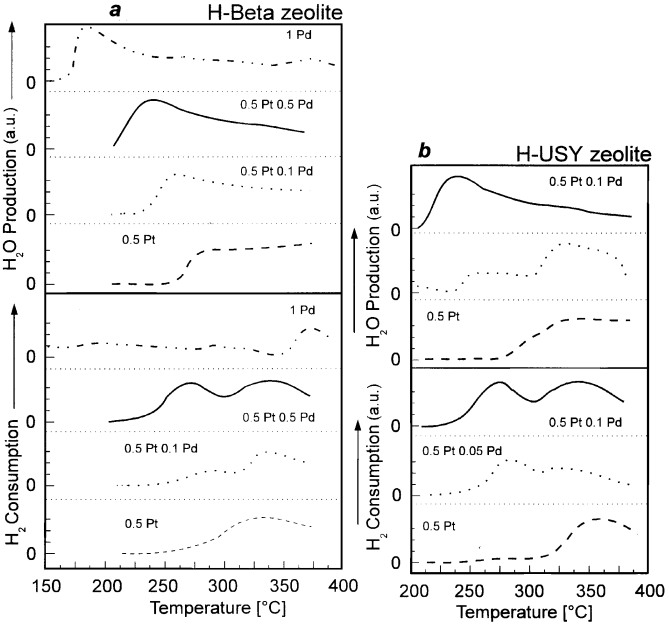

FIG. 4. Concentration of water and hydrogen in the reactor outlet (arbitrary units) during TPR of *1 $Pd^{[EX]}$H-Beta, 0.50 $Pt^{[EX]}$H-Beta* with addition of 0.0, 0.1, and 0.5 wt% of Pd ***(a)*** and during TPR of *0.50 $Pt^{[EX]}$USY* with addition of 0.0, 0.05 and 0.10 wt% of Pd ***(b)***. The samples were precalcined at 400°C in flowing oxygen.

TABLE 3

Metal Dispersion (d) and Average Metal Particle Size (D) of Pt Loaded H-Beta Zeolite, with and without Pd Addition

Metal loading	d (%)	D (nm)
1.00 Pt$^{[IM]}$	8	12
1.00 Pt$^{[EX]}$	32	3.2
1.00 Pt 0.10 Pd$^{[IM]}$	57	1.8
1.00 Pt 0.10 Pd$^{[EX]}$	59	1.7

typical for palladium being absent. The consumption of hydrogen in the temperature range 250–300°C increases with increasing Pd content of the Pt,Pd catalyst. In the USY zeolite, the combination of a small quantity of Pd (0.05 wt%) with 0.50 wt% Pt leads to significant hydrogen consumption in the 250–300°C temperature step. Palladium seems to catalyze the reduction of at least part of the platinum. Actually it is not known whether the two metals behave as an alloy, or whether they occur as separate phases in the zeolite pores.

Metal dispersions determined by hydrogen chemisorption on Pt/H-Beta catalysts with and without Pd addition are compared in Table 3. Loading of H-Beta with 1.0 wt% of Pt via impregnation leads to a low Pt dispersion of ca. 8%. Similar low Pt dispersions on Pt/H-Beta zeolites prepared this way have been observed by others (33). The use of the ion exchange technique instead of impregnation results in 32% dispersion. Addition of 0.10 wt% of Pd results in a significant improvement of the dispersion irrespective of the metal loading technique. The metal dispersions measured on *1.00 Pt 0.10 Pd$^{[IM]}$H-Beta* and *1.00 Pt 0.10 Pd$^{[EX]}$H-Beta* are very similar (57% and 59%, respectively). With bimetallic catalysts, the method of metal deposition does not seem to play an important role. Incipient wetness impregnation as well as the ion exchange technique to deposit Pt and Pd yield catalysts with substantially higher metal dispersions compared to monometallic Pt catalysts (Table 3). The origin of the higher Pt dispersion obtained in the presence of Pd is probably the lower reduction temperature (Fig. 4) limiting suiterings. *The average platinum partial size 1.00 Pt 0.10 Pd$^{[IM]}$H-Beta* and *1.00 Pt 0.10 Pd$^{[EX]}$H-Beta* catalysts is 1.7 nm. This diameter is larger than that of the pores of zeolite Beta, which is smaller than 0.7 nm. This does not necessarily mean that the noble metal is outside the zeolite micropores. Carvill *et al.* have demonstrated that the growth of platinum particles can lead to a local destruction of the zeolite (34).

1.00 Pt 0.10 Pd$^{[IM]}$H-Beta and *1.00 Pt 0.10 Pd$^{[EX]}$H-Beta* catalysts were subjected to several oxidation–reduction cycles using the conditions for fresh catalyst pretreatment. After each oxidation–reduction cycle, the Pt dispersion was determined. The high metal dispersion reached after the first activation procedure is maintained in the subsequent redox cycles. The method of metal deposition does not influence this behavior.

CONCLUSIONS

Compared to monometallic Pd/H-Beta and Pt/H-Beta zeolites, bimetallic PtPd/H-Beta zeolites are superior bifunctional catalysts for heptane isomerization. The use of the Pt–Pd metal combinations leads to a higher catalytic activity, higher yields of total C_7 isomers, as well as higher yields of multibranched C_7 isomers. This improvement is due to a better balance and intimacy of the catalytic functions. Platinum is a more active hydrogenation–dehydrogenation function, compared to palladium but the realization of sufficient dispersion with current catalyst preparation techniques is problematic. The large platinum particles catalyze heptane hydrogenolysis and the lack of intimacy favors dimerization-cracking at the acid sites. In Pt/H-Beta, the addition of as little as 20 mole% of palladium leads to a significant improvement of the platinum dispersion. Temperature programmed reduction experiments tend to indicate that the beneficial effect of Pd addition is due to a catalytic effect of this element on Pt reduction and a rapid "fixation" of the metal phase in highly dispersed form.

The beneficial effect of palladium addition on Pt dispersion of H-Beta zeolites is maintained after multiple oxidation/reduction treatments.

With USY zeolites, similar observations with respect to the improvement of catalytic properties were made, although the influence of Pd addition was less pronounced. This is probably due to the lower acidity of this zeolite.

ACKNOWLEDGMENTS

This work is part of the Ph.D. of E.B., sponsored by Shell Research B.V. J.A.M. acknowledges the flemish NFWO for a position as Senior Research Associate. A research grant from the Belgian Government within the IUAP-PAI frame is highly appreciated.

REFERENCES

1. Coonradt, M. L., and Garwood, W. E., *Ind. Eng. Chem. Prod. Res. Dev.* **3**, 38 (1964).
2. Weisz, P. B., *Adv. Catal.* **13**, 137 (1962).
3. Pichler, H., Schultz, H., Reitmeyer, H. O., and Weitkamp, J., *Erdöl, Kohle Erdgas Petrochem.* **25**, 494 (1972).
4. Weitkamp, J., *Erdöl, Kohle Erdgas Petrochem.* **31**, 13 (1978).
5. Maxwell, I. E., and Stork, W. H. J., *Stud. Surf. Sci. Catal.* **58**, 571 (1991).
6. Jacobs, P. A., and Martens, J. A., *Stud. Surf. Sci. Catal.* **58**, 445 (1991).
7. Martens, J. A., Tielen, M., Jacobs, P. A., and Weitkamp, J., *Zeolites* **4**, 98 (1984).
8. Guisnet, M., Alvarez, F., Giannetto, G., and Perot, G., *Catal. Today* **1**, 415 (1987).
9. Alvarez, F., Ribeiro, F. R., Giannetto, G., Chevalier, F., Perot, G., and Guisnet, M., *Stud. Surf. Sci. Catal.* **49**, 1339 (1989).
10. Weitkamp, J., *Ind. Eng. Chem. Prod. Res. Dev.* **21**, 550 (1982).
11. Blomsma, E., Martens, J. A., and Jacobs, P. A., *J. Catal.* **155**, 141 (1995).
12. Blomsma, E., Martens, J. A., and Jacobs, P. A., *J. Catal.* **159**, 000 (1996).
13. Blomsma, E., Martens, J. A., and Jacobs, P. A., "Proceedings, 11th Int. Zeolite Conf., Seoul, Korea, 1996."

14. Martens, J. A., and Jacobs, P. A., *in* "Theoretical Aspects of Heterogeneous Catalysis" (J. B. Moffat, Ed.), p. 52. Van Nostrand Reinhold, New York, 1990.
15. Lopéz Agudo, A., Asensio, A., and Corma, A., *J. Catal.* **69**, 274 (1981).
16. Giannetto, G., Perot, G., and Guisnet, M., *Stud. Surf. Sci. Catal.* **20**, 265 (1985).
17. Ward, J. W., *Fuel Processing Technology* **32**, 55 (1993).
18. Dowden, D. A., "Catalysis," Vol. 2 (C. Kemball and D. A. Dowden, Eds.), p. 1. The Chemical Society, London, 1977.
19. Biloen, P., Helle, J. N., Verbeek, H., Dautzenberg, F. M., and Sachtler, W. M. H., *J. Catal.* **63**, 112 (1980).
20. Gault, F. G., Zahraa, O., Dartigues, J. M., Maire, G., Peyrot, M., Weisang, E., and Engelhardt, P. A., "Proceedings, 7th Inter. Congr. Catal. Tokyo, 1981" (T. Seiyama and K. Tanabe, Eds.), Vol. 1, p. 199.
21. Maire, G. L. C., and Garin, F. G., "Catalysis," Vol. 6 (J. R. Anderson and M. Boudart, Eds.), p. 161. Springer-Verlag, Berlin/Heidelberg, 1984.
22. Ciapetta, F. G., and Wallace, D. N., *Catal. Rev.* **5**, 67 (1971).
23. Giannetto, G., Perot, G., and Guisnet, M., *Stud. Surf. Sci. Catal.* **20**, 265 (1985).
24. Guerin, M., Kappenstein, C., Alvarez, F., Giannetto, G., and Guisnet, M., *Appl. Catal.* **45**, 325 (1988).
25. Reagan, W. J., Chester, A. W., and Kerr, G. T., *J. Catal.* **69**, 89 (1981).
26. Gallezot, P., *Catal. Rev. Sc. & Eng.* **20**, 121 (1979).
27. Gallezot, P., Alarcon-Diaz, A., Dalmon, J. A., Renouprez, A., and Imelik, B., *J. Catal.* **39**, 334 (1975).
28. Chmelka, B. F., Riosin, R. R., Went, G. T., Bell, A. T., Radke, C. J., and Petersen, E. E., *Stud. Surf. Sci. Catal.* **49**, 995 (1989).
29. Chmelka, B. F., Went, G. T., Csensits, R., Bell, A. T., Petersen, E. E., and Radke, C. J., *J. Catal.* **144**, 506 (1993).
30. Ostgard, D. J., Kustov, L., Roeppelmeier, K. R., and Sachtler, W. M. H., *J. Catal.* **133**, 342 1992.
31. Zheng, J., Dong, J., and Qin-Hua, X., *Stud. Surf. Sci. Catal.* **84**, 1641 (1994).
32. Sachtler, W. M. H., *Catal. Today* **15**, 419 (1993).
33. Smirniotis, P. G., and Ruckenstein, E., *J. Catal.* **140**, 526 (1993).
34. Carvill, B. T., Lerner, B. A., Adelman, B. J., Tomczak, D. C., and Sachtler, W. M. H., *J. Catal.* **144**, 1 (1993).